Structure−Activity Relationship of 6-Methylidene Penems Bearing Tricyclic Heterocycles as Broad-Spectrum β-Lactamase Inhibitors: Crystallographic Structures Show Unexpected Binding of 1,4-Thiazepine Intermediates

Aranapakam M. Venkatesan,[†] Yansong Gu,[†] Osvaldo Dos Santos,[†] Takao Abe,[‡] Atul Agarwal,[†] Youjun Yang,[†] Peter J. Petersen,[†] William J. Weiss,[†] Tarek S. Mansour,*[,†] Michiyoshi Nukaga,[§] Andrea M. Hujer,[∥] Robert A. Bonomo,[∥] and James R. Knox*[,§]

Wyeth Research, 401 N. Middletown Road, Pearl River, New York 10965, Wyeth Lederle Japan, Saitama, Japan, Department of Molecular and Cell Biology, The University of Connecticut, Storrs, Connecticut 06269-3125, and Research Service, Department of Veterans Affairs Medical Center, Cleveland, Ohio 44106

Received April 30, 2004

The design and synthesis of a series of seven tricyclic 6-methylidene penems as novel class A and C serine β-lactamase inhibitors is described. These compounds proved to be very potent inhibitors of the TEM-1 and AmpC β-lactamases and less so against the class B metallo-β-lactamase CcrA. In combination with piperacillin, their in vitro activities enhanced susceptibility of all class C resistant strains from various bacteria. Crystallographic structures of a serine-bound reaction intermediate of **17** with the class A SHV-1 and class C GC1 enzymes have been established to resolutions of 2.0 and 1.4 Å, respectively, and refined to *R*-factors equal 0.163 and 0.145. In both β-lactamases, a seven-membered 1,4-thiazepine ring has formed. The stereogenic C7 atom in the ring has the *R* configuration in the SHV-1 intermediate and has both *R* and *S* configurations in the GC1 intermediate. Hydrophobic stacking interactions between the tricyclic C7 substituent and a tyrosine side chain, rather than electrostatic or hydrogen bonding by the C3 carboxylic acid group, dominate in both complexes. The formation of the 1,4- thiazepine ring structures is proposed based on a *7-endo-trig* cyclization.

Introduction

β-Lactamases are enzymes that hydrolyze β-lactam rings in all classes of β-lactam antibiotics. The production of such enzymes by bacteria is the most common resistance mechanism against β-lactam antibiotics, a matter that constitutes a major threat to human health. β-Lactamases can be either plasmid-mediated, such as class A TEM enzymes, or chromosomal represented by class C AmpC enzymes.[1] It is estimated that amoxicillin resistance in Gram-negative *Escherichia coli* bacteria amounts to 50% of isolates in hospitals, whereas penicillin resistance to Gram-positive *Staphylococcus aureus* bacteria reaches over 90% of clinical isolates.[2] Therefore, the intensive search for a new generation of inhibitors with broader spectrum of activity than clinically used clavulanic acid, sulbactam, and tazobactam continues unabated. This search is especially important given the fact that these heavily used inhibitors are becoming ineffective against newly appearing mutant β-lactamases.

Previous work reported on methylidene β-lactam antibiotics has focused mostly on monocyclic rings attached to the exocyclic double bond linkage of penems,[3−6] cephems,[7] and extended carbon derivatives[8] (Figure 1). Investigations in our laboratories have identified penam sulfones,[9] spirocyclopropyl penam sulfones,[10] and methylidene penems[11] as mechanism-based inhibitors of serine-reactive class A and C β-lactamases, whereas others reported transition-state analogue inhibitors.[1b,i] High-resolution crystallographic structure determination of an inhibitor with class A and C β-lactamases describing the mode of action of imidazo-[2,1-*c*][1,4]oxazin methylidene penem **7** established the formation of a novel seven-membered 1,4 thiazepine intermediate having R stereochemistry at the C7 moiety.[12] However, an unexpected feature reported in this study indicated that the 1,4-thiazepine intermediate is oriented differently in each complex following the acylation reaction between **7** and active serine residue. This finding is significant in the context of designing new analogues with desired potency against both class A and C enzymes. Accordingly, on the basis of these findings, we undertook the synthesis and biological evaluation of novel tricyclic methylidene penems **11**−**17**, followed by the crystallographic structure determination of reaction intermediates of **17** with the SHV-1 and GC1 β-lactamases, which are well-characterized members of the class A and C families. It is found that the 1,4-thiazepine intermediate has distinctive hydrophobic contacts within the binding site of each β-lactamase.

Chemistry

The tricyclic 6-methylidene penem carboxylic acid sodium salts **11**−**17** were prepared by a two-step process, starting from (5*R*,6*S*)-6-bromo-7-oxo-4-thia-1-azabicyclo[3.2.0]hept-2-ene-2-carboxylic acid 4-nitrobenzyl ester **9**, which was prepared from the commercially available 6-aminopenicilanic acid (6-APA) **8** by a multistep procedure modified[13] from the previously available procedure.[14]

* To whom correspondence should be addressed. T.S.M.: Tel, (845) 602-3668; Fax, (845) 602-5580; E-mail, mansout@wyeth.com. J.R.K.: Tel, (860) 486-3133; Fax, (860) 486-4745; E-mail, james.knox@uconn.edu.
[†] Wyeth Research.
[‡] Wyeth Lederle Japan.
[§] The University of Connecticut.
[∥] Department of Veterans Affairs Medical Center.

10.1021/jm049680x CCC: $27.50
Published on Web 11/18/2004

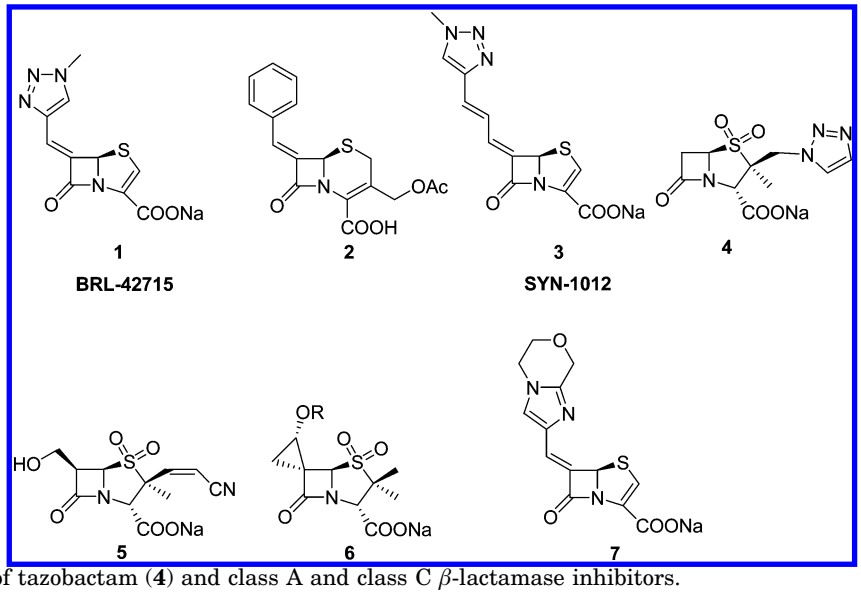

Figure 1. Structure of tazobactam (**4**) and class A and class C β-lactamase inhibitors.

Scheme 1. General Method To Prepare Compounds **11-17**

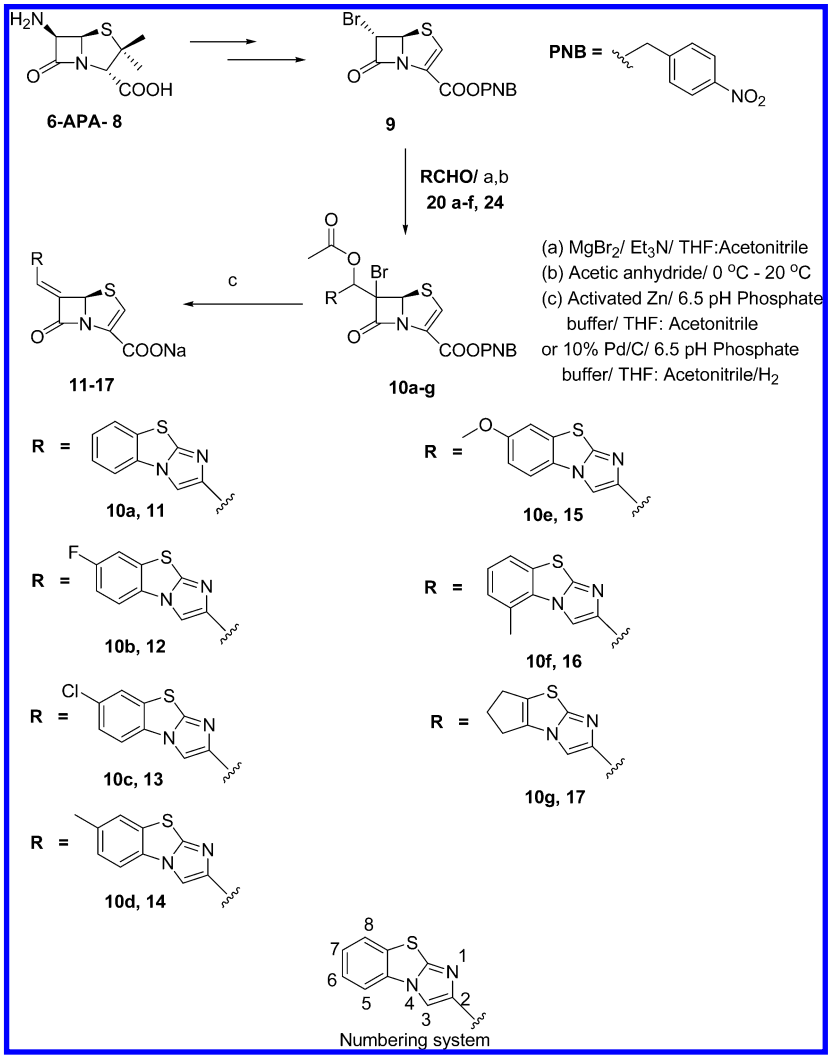

The first step involved a Lewis acid mediated aldol condensation between **9** and the appropriately substituted aldehydes **20a**−**f** and **24** in the presence of anhydrous $MgBr_2$ and triethylamine (Scheme 1). Previously, this transformation was carried out using strong lithium bases such as lithium diisopropylamide, (LDA) lithium hexamethyldisilazide (LHMDS), or Ph_2NLi with PMB ester group, which led to poor yields and unpredicted side products.[15]

The aldehydes **20a**−**f** were prepared starting from the commercially available 2-aminobenzothiazole derivatives **18**. The appropriately substituted 2-aminoben-

Scheme 2. Synthesis of Aldehydes **20a**−**f**

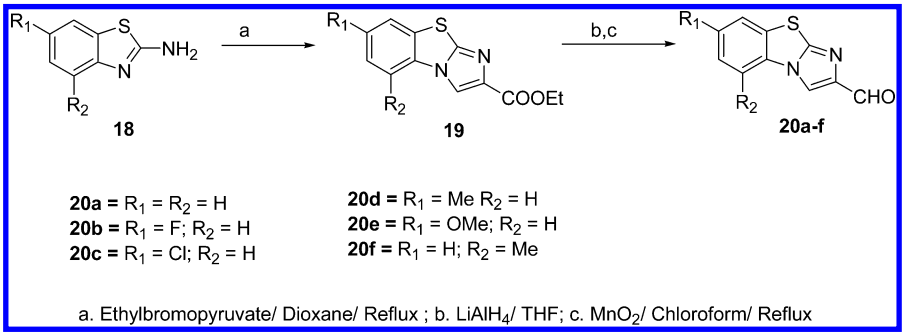

Scheme 3. Synthesis of Aldehyde **24**

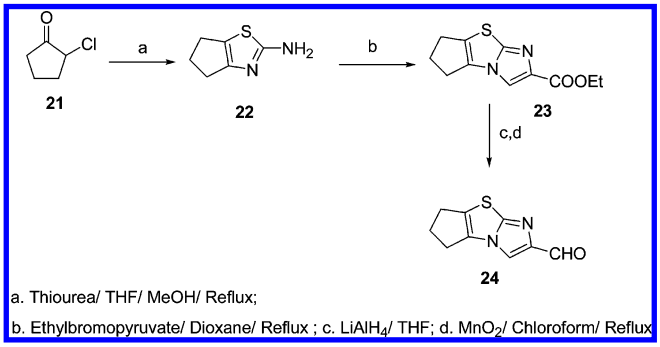

Table 1. In Vitro Activity of Compounds **11**−**17** against Different β-Lactamases

	IC$_{50}$, nM	
compound	TEM-1	AmpC
tazobactam	100 ± 8	84,000 ± 300
11	10.0 ±2	1.0 ± 0.5
12	8.0 ± 1	2.0 ± 1
13	6.0 ± 1	3.0 ± 1
14	3.0 ± 1	1.0 ± 0.5
15	18.0 ± 2	2.0 ± 1
16	9.0 ± 2	2.0 ± 1
17	1.0 ± 0.4	2.0 ± 1

Table 2. In Vitro Activity of Compounds **11**−**17** against CcrA

compound	IC$_{50}$, nM	compound	IC$_{50}$, nM
tazobactam	400,000 ± 200	14	103 ± 9
11	350 ± 6	15	250 ± 5
12	370 ± 5	16	370 ± 8
13	74 ± 3	17	240 ± 6

zothiazole derivatives were reacted with ethyl bromopyruvate in dimethoxyethane. The resulting tricyclic ester derivatives were reduced to their corresponding alcohols using $LiAlH_4$ and oxidized to their respective aldehydes **20a**−**f** using active MnO_2 in refluxing chloroform for 48 h (Scheme 2). The aldehyde **24** was prepared by a Hantzch reaction in which α-chlorocyclopentanone was reacted with thiourea to afford the 2-aminothiazole derivative **22**. This was converted to aldehyde **24** by the sequence of reactions described for the preparation of compounds **20a**−**f** and shown in Scheme 3.

Results and Discussion

Structure−**Activity Relationship.** The in vitro inhibitory activities (IC$_{50}$ values in nM) for all the newly synthesized compounds **11**−**17** are shown in Tables 1 and 2. As mentioned earlier, all seven compounds were tested against TEM-1 (class A), CcrA (class B), and AmpC (class C) β-lactamases. In comparison with tazobactam, the new inhibitors exhibited excellent activity against the enzymes listed here. These compounds were very potent inhibitors of TEM-1 and AmpC enzymes with IC$_{50}$ values in the range of 1−18 and 1−3 nM, respectively. Furthermore, in comparison to tazobactam, they exhibited almost 5−100 fold greater potency against TEM-1 enzyme and were about 28,000−84,000-fold more potent against AmpC enzymes. Within this series of new inhibitors, comparison of their potencies reveals that any substitution on the aromatic ring or any modification did not alter their potency against the AmpC enzyme significantly. However, the substitution on the 7-position (see the numbering in Scheme 1) of the heterocycle alters the potency against the TEM-1 enzyme slightly. Replacement of hydrogen on the 7-position of the heterocycle with fluorine (compound **12**) or chlorine (compound **13**) does not change their potencies dramatically. However, the presence of a methyl group at position 7 (compound **14**) increased the potency against TEM-1 by 2-fold. Moving the methyl from the 7 to the 5 position (compounds **14** and **16**) led to a drop in the potency against TEM-1. This loss in potency was recovered by changing the aromatic ring of compounds **11**−**16** to an alicyclic ring (compound **17**), which increased the potency against TEM-1 by 10 fold. To expand further their spectrum of activity, compounds **11**−**17** were found to be good inhibitors of the class B metalloenzyme CcrA in comparison to tazobactam (Table 2).

Further in vitro evaluation in cell-based assay (MIC) reaffirmed the effectiveness of compounds **11**−**17** as potent broad spectrum β-lactamase inhibitors. These data are summarized in Table 3, which also lists the expressing enzyme and its class. In all these experiments, piperacillin was combined with the newly synthesized inhibitors and tested against various piperacillin-resistant pathogens (MIC < 64 μg/mL) expressing different β-lactamases. The piperacillin + tazobactam combination was used as a comparator. At the onset, it is important to note that when tested alone, both tazobactam and the 6-methylidene penem inhibitors **11**−**17** did not exhibit any antibacterial activity, which confirmed the fact that these compounds do not have any intrinsic antibacterial activity. When combined with piperacillin, compounds **11** and **17** are as active as tazobactam against class A producing *E. coli* pathogens. In these cases the MIC values of the weaker inhibitor **15** in combination with piperacillin was found to be higher than that of other inhibitors, which is consistent with the IC$_{50}$ values reported against TEM-1. The permeability in *E. coli* is evaluated with the permeable

Table 3. In Vitro Antimicrobial Activity of Inhibitors[a] **11**−**17** in Combination with Piperacillin (Pip) at a Constant 4 μg/mL Concentration

species & strain	expression	Tazo[a] + Pip	**11** + Pip	**12** + Pip	**13** + Pip	**14** + Pip	**15** + Pip	**16** + Pip	**17** + Pip
E. coli GC 2844	none	2	2	2	2	2	2	2	2
E. coli GC 2847	TEM-1 (class A)	2	2	8	4	4	16	8	4
E. coli GC 2920	IRT-2 (class A)	4	2	2	1	2	2	2	2
E. coli GC 2804	Imp	0.12	<0.06	<0.06	<0.06	<0.06	<0.06	<0.06	<0.06
E. coli GC 2805	CcrA (class B)	>64	>64	>64	>64	>64	>64	>64	>64
E. coli GC 2252	IRT-2 (class A)	2	8	16	16	16	8	16	8
E. cloacae GC 1477	AmpC (class C)	>64	16	32	16	32	64	32	16
E. cloacae GC 2071	Imi+1 + AmpC (class A+C)	>64	2	8	8	8	16	16	4
E. cloacae GC 1475	P99 (class C)	>64	8	16	8	8	16	16	16
K. pneumoniae GC 2825	four enzymes (not characterized)	>64	16	16	32	8	64	16	4
S. marcescens[b] GC 1781	Sme-1 + AmpC	1	0.50	2	1	0.50	2	4	1
P. aeruginosa[c] GC 1764	AmpC	>64	4	4	16	16	32	2	2
S. marcescens GC 4142	AmpC	>64	1	2	2	1	2	4	2
E. coli GC 2203	control	>64	2	2	1	1	1	2	2
S. aureus GC 2216	control	64	<0.06	<0.06	<0.06	<0.06	<0.06	<0.06	2

[a] Tazo = tazobactam. [b] *S. marcescens* = *Serratia marcescens*. [c] *P. aeruginosa* = *Pseudomonas aeruginosa*.

strain 2804, where all inhibitors had potent activity. Therefore, this aspect should be taken into consideration in assessing the in vitro activity against strains from different bacteria.

It should be noted from Table 3 that even though the tazobactam + piperacillin combination is potent against class A producing pathogens, this combination is less effective against class C producing organisms, such as *Enterobacter cloacae* GC 1477, GC 2071, and GC 1475. However, the addition of the inhibitors **11**−**17** restored susceptibility to piperacillin for 100% of the class C producing strains listed here, including *Klebsiella pneumoniae* GC2825, which expresses four uncharacterized β-lactamases. However, all inhibitors **11**−**17** were ineffective against *E. coli* GC 2805 (a class B producing bacteria) due to their moderate activity against CcrA. Due to its potent activity, compound **17** was chosen to elucidate the mechanism of inhibition by X-ray crystallographic techniques using SHV-1 (class A) and the extended-spectrum GC1 (class C) enzymes. Against SHV-1 and GC1, compound **17** was determined to have an IC_{50} value of 12 and 3.8 nM, respectively.

Structure Determination of the Enzyme Complexes. Rigid-body refinement using the unliganded SHV-1 (PDB entry 1SHV) and GC1 (PDB entry 1GCE) β-lactamases was done at 2 Å with CNS.[16] *R*-factors were ca. 35% for the unsolvated apoprotein models. A simulated annealing protocol and cross-validation[17] were then used in the refinements. XtalView[18] was employed for map displays and for manipulation of the structures. As the protein models were being optimized, a serine-bound structure was evident in the difference density of both complexes. On the basis of previous crystallographic work on the related penem **7**,[12] species **28** and **29**, the chiral forms of species **27** (Scheme 4), were added to the model of each complex. Because the 7-atom ring in **27** has three tautomeric forms, only weak refinement restraints were applied to the ring geometry. In the case of the GC1 complex, two conformers of the intermediate were introduced in later refinement steps. The last stage of the higher resolution refinement of GC1 was performed with SHELX[19] using all data (Table 1, Supporting Information). At 1.4 Å resolution, the introduction of anisotropic *B*-factors reduced the *R* and R_{free} values by 3.5% and 1.1%. Riding hydrogen atoms were later added in calculated positions.

Figure 2 shows the mixed α−β tertiary structure of each β-lactamase molecule. Ramachandran analysis of the SHV-1 and GC1 protein backbone showed 92.0% and 92.3% of residues, respectively, fall in most favored regions, with none in disallowed regions. Residues 214−217 in the Ω loop (residues 200−226) of GC1 were not clear and were not modeled. The difference electron density of reaction intermediate **27** in each enzyme is shown in Figure 3.

The absolute configuration at carbon C7 (initially C6′) is variable in the two complexes. A single conformer **28** with the *R* configuration is observed in the SHV complex, whereas in the GC1 complex the conformer with the *R* configuration has only 30% occupancy and coexists with the predominant *S* conformer (70%) **29**. It is possible that both stereoisomers are formed initially in each β-lactamase, but the form more stable to hydrolysis predominates in the crystallographic maps. Alternatively, stereospecific reaction pathways may differ in each active site, producing one chiral form in preference to the other. The C3 carboxylic acid group of the minor R conformer was not well-defined in the GC1 map and was not modeled.

Inhibitor-Induced Changes in the Enzyme Structures. When the SHV-1 complex is superposed over the crystal structure of the uninhibited β-lactamase,[20] several changes are seen. The side chain of Tyr105 reorients slightly (15°−20°) to sandwich stack with the C7 heterocyclic substituent of the inhibitor (Figure 4). Its closest contact (ca. 3.5 Å) is with the terminal ring of the tricyclic substituent. The binding site widens slightly so that the distance from the 104−106 loop to the B3 β-strand (234−238) increases by nearly 1 Å. Conserved Glu166 and its hydrogen-bonded water molecule, important for catalysis, are now closer (2.4 Å) than in the apoenzyme. This short distance may be an artifact due to vibration or disorder in either or both groups.

Overlay of the GC1 complex with the uninhibited enzyme[21] shows little indication of a second Ω-loop pathway seen in other GC1 complexes.[12,22] Tyr224 in the loop is sandwiched with the tricyclic substituent of the predominant *S* conformer of the inhibitor intermediate. The side chain of Gln120 is found in two rotameric conformations about Cα−Cβ, one pointing outward and the other directed inward to hydrogen bond with the N atom of the imidazoyl ring in the tricyclic substituent.

Scheme 4. Mechanism of Inhibition of SHV-1 and GC1 β-Lactamases by **17**[a]

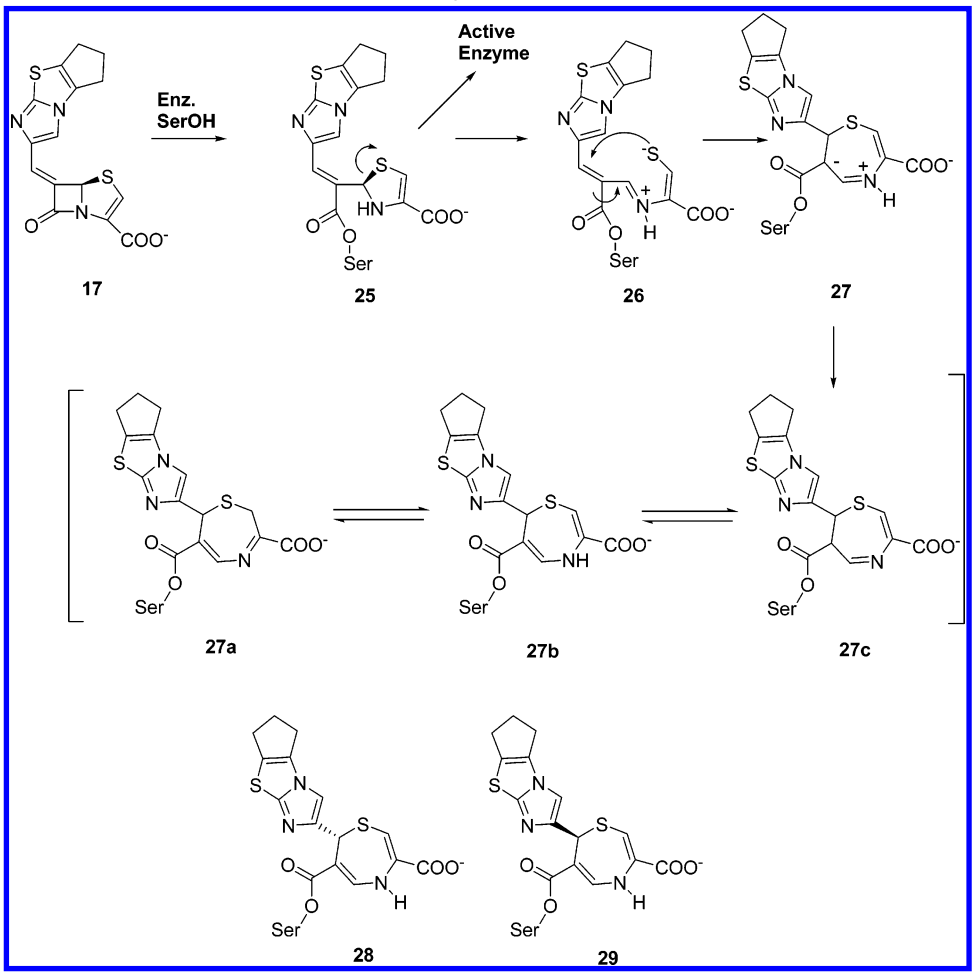

[a] Species **27** is observed in the crystal structures of both enzymes.

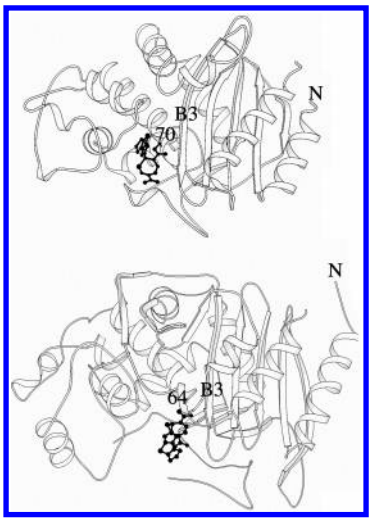

Figure 2. Tertiary structure of (a) the class A SHV-1 β-lactamase complex and (b) the class C GC1 complex. The thiazepine intermediate **27** is bound to the reactive serines 70 and 64, respectively. Four residues in the Ω loop at the bottom of the GC1 enzyme were not seen. Drawn by MOLSCRIPT.[37]

Asn152 also rotates slightly to bind with this N atom. Other changes involve the polypeptide backbone. The segment from 118 to 123 on the left of the binding site moves about 0.5 Å, and the 293−298 segment above the binding site moves about 1.4 Å, so the hydrophobic side chains of Leu119 and Leu296 shift toward the intermediate.

Mechanism of Inhibition. A proposed pathway for the conversion of penem **17** to the intermediate observed by crystallography is given in Scheme 4. Acylation of the reactive serine (Ser70 or Ser64) of the SHV-1 class A or GC1 class C β-lactamase produces species **25**, which may be very susceptible to hydrolysis.[4,31] Rotation about the C5−C6 bond and ring opening produces a reactive thiolate species **26**. Thiolate **26** undergoes a 7-endo-trig cyclization in preference to a 6-exo-trig process to produce the seven-membered thiazepine ring. The thiolate attack on the C6−C6′ double bond can occur from either side to produce chirality at carbon 7 (initially C6′). The dihydrothiazepine **27** is drawn as the ion pair of three tautomeric forms **27a**−**c**. The experimental electron density at C6 is almost planar, so we believe the amount of tautomer **27c** is small.

Orientation and Interactions of the Intermediate in Each Binding Site. In both class A and class C binding sites the serine-bound intermediate has its β-lactamyl carbonyl group hydrogen bonded to main chain amide groups of the reactive serine and β-strand B3. The positions of the 7-atom rings are generally equivalent in the two binding sites, with the exception that the ring of the minor R conformer in the class C complex is rotated ca. 180° about the bond to the serine ester.

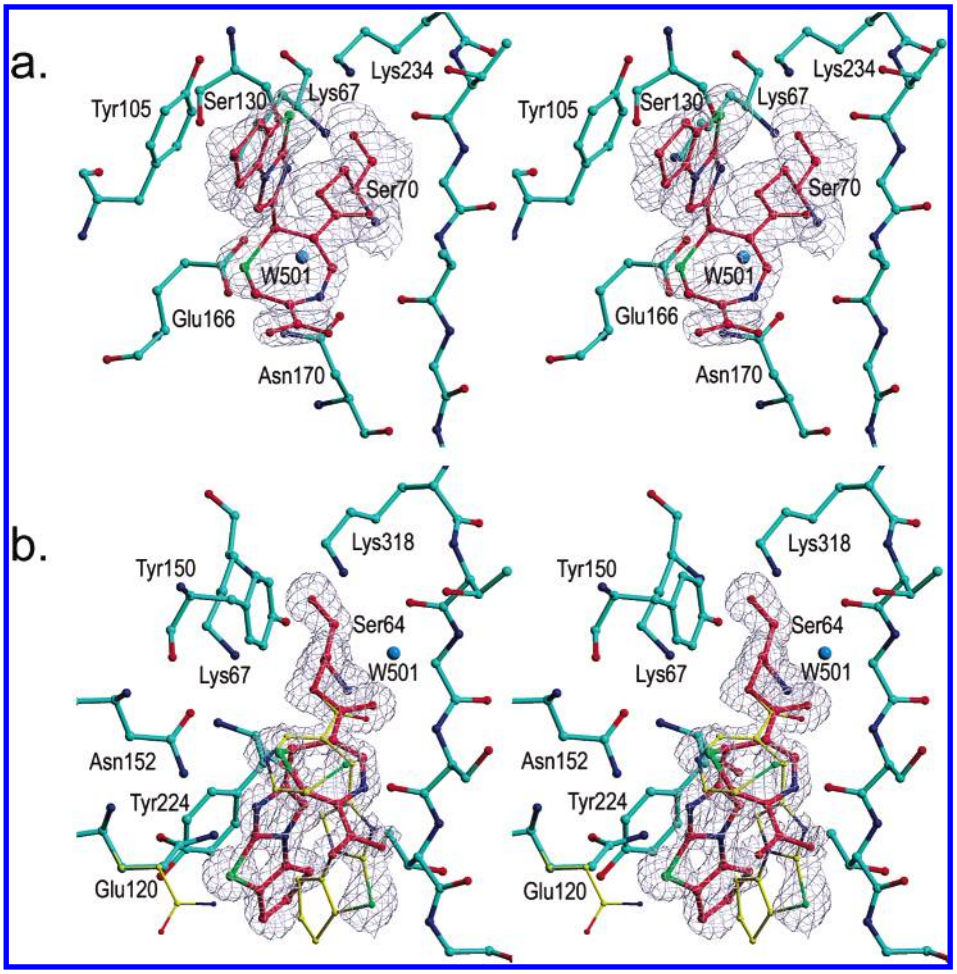

Figure 3. Stereoview of the $F_o - F_c$ electron density of the intermediate **27** bonded to the reactive serine in (a) the SHV-1 β-lactamase and (b) the GC1 β-lactamase. The density contour level is 3σ. The figure was made by XtalView[18] and Raster3D.[38]

In both complexes the C3 carboxylic acid group of the thiazepine ring is solvated and has no interactions with the enzyme. In the class A β-lactamase, the N4 atom in the thiazepine ring is 3.1 Å from, but poorly oriented to, the main chain carbonyl oxygen atom of residue 237 on the B3 β-strand. The N4 atom of the main conformer of the class C complex has no protein interactions, though in the minor conformer it is 3.2 Å from the Asn152 amide group.

The rotameric conformation of the tricyclic substituent about the C7−C heterocycle bond differs from one enzyme to the other. In the SHV-1 class A binding site, the ring edge containing the S and N atoms is directed inward toward the hydrophobic Val216 at the top of the binding site. In both conformers of the GC1 class C complex, the S−N edge of the substituent is turned outward. In the major conformer the imidazole N atom has hydrogen bonds with the amide groups of Gln120 (2.8 Å) and Asn152 (2.9 Å), while in the minor conformer the N atom has no interactions with protein.

Of possibly greater significance in the binding is a sandwich stacking of the large tricyclic ring with a tyrosine ring in each binding site. Tyr105 in the class A SHV-1 enzyme and Tyr224 in GC1 are each about 3.5 Å from the tricyclic ring. These tyrosines are almost conserved in class A and class C β-lactamases (Tyr224 is conventionally numbered 221 in wild-type sequences) but are in very different regions of the two binding sites. It would be useful to determine the generality of this stacking interaction in other complexes of each enzyme.

Hydrolysis of the Acyl Intermediate. Neither the heterocylic group nor the thiazepine ring is able to block the approach of a water molecule to the acyl ester bond, as seen in some β-lactamase complexes.[22−24] In the SHV-1 class A binding site, a water molecule activated by Glu166 is thought to attack from the relatively buried side of the ester bond[25] (Figure 3). We observe this water molecule, but the short length of its hydrogen bond indicates the presence of some disorder, which may impair efficient deacylation. In class C enzymes, the water is believed to attack from the more exposed top side of the ester. Normally, conserved Tyr150, and possibly the β-lactamyl intermediate itself,[25−27] may activate the hydrolytic water molecule.[28,29] In GC1 a molecule of water is found above but rather far (3.6 Å) from the ester bond, and the water is uninvolved with the Tyr150 hydroxyl group (4.2 Å). Substrate assistance in activating this water, via the intermediate's C3 carboxylate group or N4 nitrogen atom, is not possible here. Thus, the stability of the acyl intermediate is more readily accounted for in the GC1 class C case than in class A. Structural reasons for the disorder (SHV-1) and poor activation (GC1) of the water remain unclear. Perhaps more important, in both cases, is the large contribution to stability provided by the conjugation of the acyl ester with the large dihydrothiazepine ring

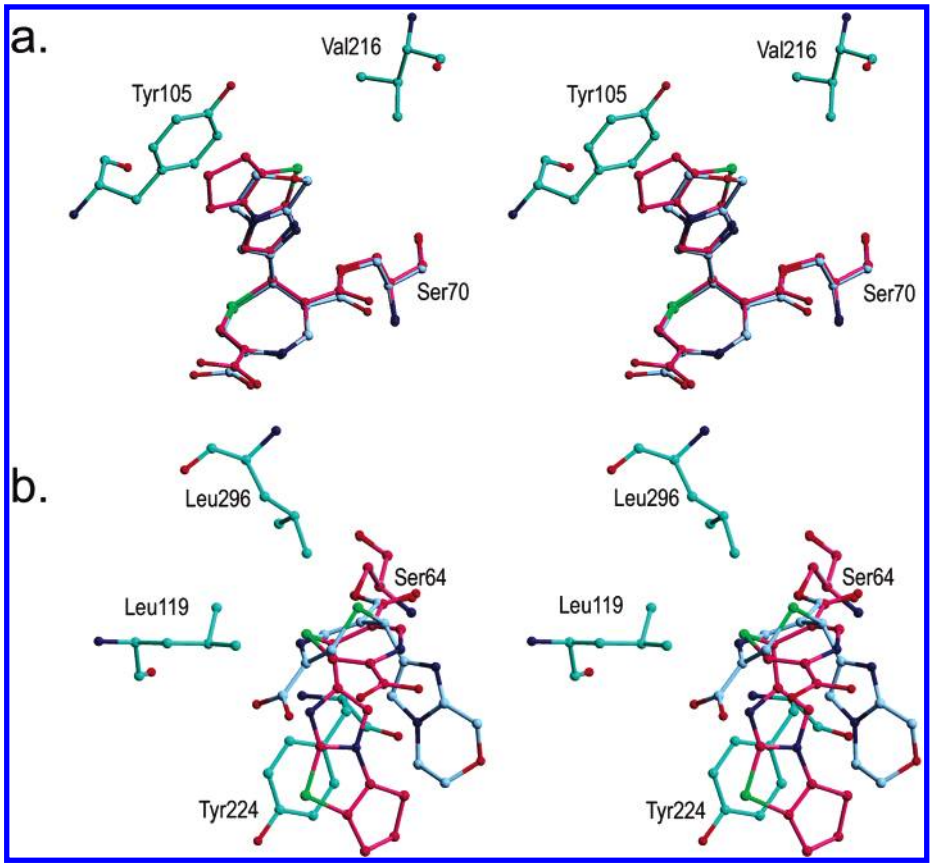

Figure 4. Stereoview of the overlay of the intermediates of **17** (red) and **7** (light blue) in (a) the class A SHV-1 β-lactamase and (b) the class C GC1 β-lactamase. Tyrosines Tyr105 or Tyr224 stack with the heterocyclic group on C7. Only the major *S* conformer of **17** is shown for the GC1 enzyme. The minor *R* conformer is near the position of **7**.

system, particularly in the vinylogous urethane tautomeric structures **27a** and **27b**.

Comparison of the Binding by Tricyclic 17 and Bicyclic 7. Our crystal structures show that both penems react to form the same thiazepine intermediate, the 7-atom rings of which overlay very closely (Figure 4). The stereoconfiguration at C7 in the complexes of these two enzymes with **7** is exclusively *R*,[12] whereas here in the complexes with **17** the *R* form is found exclusively only in the SHV-1 class A enzyme. The heterocycle of both inhibitors is found in the upper region of the SHV-1 class A binding site but in the bottom of the GC1 class C binding site. In all cases the heterocyclic group lies on the side of the thiazepine ring opposite the expected position of the hydrolytic water molecule. Thus, the rather large heterocycles do not block an attack by water on the acyl ester bond.

In the case of **17**, the conformer engaged in tyrosine stacking has higher crystallographic occupancy than the unstacked conformer. One explanation, applicable to both enzymes, is that the stacked conformer is more resistant to hydrolysis by virtue of this anchoring and fixed position. An unstacked conformer may have more degrees of freedom, some of which might better position the intermediate for hydrolysis. But this argument appears to fail in the case of **7**, where the stacked conformer is found only in the SHV-1 class A enzyme.[12] However, with **7**, the Tyr224 of the GC1 class C enzyme had two main-chain positions in the crystal structure, so that full-time stacking was not possible. Further, the bicyclic ring system in **7** is relatively less conjugated than the tricyclic system in **17**. The more conjugated **17** easily stacks with Tyr224, **7** less so.

Generally, binding by these thiazepine intermediates appears to be only marginally dependent on hydrogen bonding and electrostatics. For example, one of the expected functionalities,[4] the C3 carboxylic acid group, is solvated in most complexes and has few significant protein interactions. Rather, the hydrophobicity of the multicyclic substituent at C7 and, possibly, its degree of conjugation appear to have greater influence on the positioning of the intermediate. Optimization of the design of the C7 substituent to exploit this stacking interaction could prove beneficial.

Prior Penem Studies. A comparison can be made with earlier chemical and modeling studies of the related monocyclic penem **1**[4,5,31] All these workers predicted the expanded ring structure now observed by crystallography after the reaction of **7** or **17** with both β-lactamases. Major differences are found, however, in the predicted C7 stereochemistry of the intermediate and in its interactions with the β-lactamases. In an energy minimization study,[4] the thiazepine intermediate of **1** was docked in the binding sites of class A and class C β-lactamases. The modeling indicated that only the C7(S) conformer could be accommodated in each enzyme, and it predicted specific hydrogen-bonding interactions of the C3 carboxylic acid group, none of which are observed in our four crystal structures (ref 12 and present work). It is notable too that the tyrosine stacking interaction with the C7 heterocycle was not predicted, possibly because the methyltriazolyl group

in **1** is smaller than the bi- and tricyclic groups studied here. Nevertheless, our results emphasize that modeling the binding of acyl intermediates in these enzymes can be misleading, and they demonstrate the limitation of some docking algorithms in quantitating the weak van der Waals interactions that are often critical in complexation.

Conclusion

Novel 6-methylidene penems bearing tricyclic heterocycles were synthesized from bromopenem **9** by employing a unique aldol reaction mediated by $MgBr_2$/triethylamine followed by reductive elimination. The new penems proved to be potent inhibitors of serine-reactive class A and C β-lactamases and had excellent MIC values in combination with piperacillin. The inhibitory reaction of **17** with the SHV-1 class A and GC1 class C β-lactamases as monitored by X-ray crystallography revealed the formation of a 1,4-thiazepine intermediate with unexpected modes of binding. The significance of hydrophobic stacking of the C7 heterocycle with Tyr105 and Tyr224 in SHV-1 and GC1, respectively, and its possible role in protecting the intermediate from hydrolytic attack are presented. Both chiral forms of the intermediate were found, but with differing degrees of crystallographic occupancy in each enzyme. While C7-(*R*) is seen in both enzymes to a different extent, C7(*S*) is seen only in GC1. It is unknown whether both chiral forms are made initially in equal proportion, or stereoselectively, as one chiral form may have hydrolyzed more readily than the other. The present work together with that reported earlier[12] on a bicyclic penem discloses new insights and considerations into β-lactamase inhibition that impacts the design of new inhibitors.

Experimental Section

Biological Testing. All the compounds prepared here were tested in vitro against TEM-1 (class A), CcrA (class B), and Amp-C (class C) β-lactamases for their inhibitory activity by the spectrometric method as described by Bush et al. using nitrocefin as the substrate.[32] Homogeneously purified β-lactamases were prepared from *E. coli* (TEM-1, SHV-1), *E. cloacae* (Imi-1, AmpC, GC1), and *Bacteroides fragilis* (CcrA). The enzyme concentrations were 4.4 nM (TEM-1), 31 nM (SHV-1), 1.2 nM (CcrA), 2.1 nM (AmpC), and 5.7 nM (GC1), respectively. The maximal residual velocity was then measured.

After testing these compounds for the enzyme inhibition assay, the test compounds were subjected to the whole cell in vitro susceptibility testing assay. The in vitro activities, as minimum inhibitory concentrations (MIC's), were obtained by the microbath dilution method.[33] MIC values were determined for the combination of inhibitor with piperacillin (Pip) at a constant concentration of 4 μg/mL of the inhibitor.

Subcloning and Protein Purification. The SHV-1 β-lactamase gene (bla_{SHV-1}, GenBank AF124984) was directionally subcloned into pBCSK from a clinical strain of *K. pneumoniae* 15571.[34] *E. coli* DH10B was used to harvest the SHV-1 enzyme.[20] The *E. cloacae* GC1 enzyme, a natural extended-spectrum variant of the *E. cloacae* wild-type P99 enzyme, was obtained from the GC1 β-lactamase gene on the pCS101 plasmid in *E. coli* AS226-51, as previously described.[21,35]

Crystallization of the Apo β-Lactamases. SHV-1 crystals were grown from PEG (M_r = 6000) as previously described.[20] The 28.9 kDa SHV-1 enzyme crystallizes in $P2_12_12_1$ with one molecule in the asymmetric unit. The β-lactamase from *E. cloacae* GC1 was crystallized in PEG (M_r = 8000) at pH 7.[21] The GC1 crystals have space group $P2_12_12$ with one molecule of 39.4 kDa in the asymmetric unit.

Reaction with Penem Inhibitor. A crystal of SHV-1 was soaked at 21 °C for 3 h in a 30% PEG holding solution (pH 7) containing 10 mM of **17**. The inhibitor solution was refreshed 15 min before crystal cooling and X-ray data collection. A crystal of the GC1 enzyme was soaked with 2 mM **17** for 70 min.

X-ray Data Collection. For cryoprotection, the inhibitor-soaked SHV-1 and GC1 crystals were immersed for 10−15 s in a solution containing 25% MPD or 25% glycerol, respectively, in the PEG holding solution. Crystals were flash-cooled at 100 K with a nitrogen gas stream. For SHV-1, data were collected on a Bruker HISTAR multiwire area detector on a Rigaku RU-200 X-ray generator (λ = 1.542 Å) with double-mirror Franks focusing. Frames were counted for 2 min through an ω range of 0.2° and were processed with XGEN (Molecular Simulations, Inc.). For GC1, 1° oscillation images were collected on a Q210 CCD detector (Area Detector Systems Corp.) at station A1 of the Cornell High Energy Synchrotron Source (MacCHESS). The HKL programs[36] were used to process GC1 intensities. Results are given in Table 2 of the Supporting Information. Atomic coordinates and structure factors have been deposited in the Protein Data Bank at the Research Collaboratory for Structural Bioinformatics at Rutgers University (entries 1Q2P and 1Q2Q for the SHV and GC1 complexes, respectively).

General Methods. Melting points were determined in open capillary tubes on a Meltemp melting point apparatus and are uncorrected. ^{1}H NMR spectra were determined with a Bruker DPX-400 spectrometer at 400 MHz. Chemical shifts δ are reported in parts per million (δ) relative to residual chloroform (7.26 ppm), TMS (0 ppm), or dimethyl sulfoxide (2.49 ppm) as an internal reference with coupling constants (J) reported in hertz (Hz). The peak shapes are denoted as follows: s, singlet; d, doublet; t, triplet; q, quartet; m, multiplet; br, broad. Electrospray (ES) mass spectra were recorded in positive or negative mode on a Micromass Platform spectrometer. Electron impact and high-resolution mass spectra were obtained on a Finnigen MAT-90 spectrometer. Combustion analysis was obtained using a Perkin-Elmer Series II 2400 CHNS/O analyzer. Chromatographic purifications were performed by open chromatography using IBW-127ZH (Fuji Silysia). Thin-layer chromatography (TLC) was performed on Merck PLC prescored plates $_{60}F_{254}$.

The terms "concentrated" and "evaporated" refer to removal of solvents using a rotary evaporator at water aspirator pressure with a bath temperature equal to or less than 40 °C. Unless otherwise noted, reagents were obtained from commercial sources and were used without further purification. All the substituted and unsubstituted ethylimidazo[2,1-*b*]-benzothiazole-2-carboxylates were prepared by the known literature procedure.[39] The esters were reduced to alcohols and the crude products (after characterizing them using mass-spectra) were taken to the next step to prepare novel aldehydes **20a**−**f** and **24**.

Preparation of (5*R*,6*Z*)-6-(Imidazo[2,1-*b*][1,3]benzothiazol-2-ylmethylene)-7-oxo-4-thia-1-azabicyclo[3.2.0]hept-2-ene-2-carboxylic Acid Sodium Salt (11). Step 1: Ethyl Imidazo[2,1-*b*]benzthiazole-2-carboxylate. Ethyl bromopyruvate (9.8 g, 50 mmol) was added dropwise to a stirred solution of 2-aminobenzothiazole (7.5 g, 50 mmol) in dimethoxyethane (100 mL) at room temperature. After the addition, the reaction mixture was heated to reflux for 6 h. The reaction mixture was cooled to room temperature and quenched with ice cold water. The aqueous layer was neutralized with NH_4-OH and the separated solid was filtered. It was washed well with water and dried. The crude product was purified by silica gel column chromatography by eluting it with 75% ethyl acetate:hexane: brown solid; yield 10 g, 81%; mp 97 °C; MS $(M + H)^+$ 248.

Step 2: Imidazo[2,1-*b*]benzthiazole-2-methanol. To a stirred slurry of $LiAlH_4$ (2.0 g, excess) in dry THF was slowly added ethyl imidazo[2,1-*b*]benzthiazole-2-carboxylate (4.9 g, 20 mmol) in THF (100 mL) at 0 °C. After the addition, the reaction mixture was stirred at room temperature for 1 h and quenched with saturated NH_4Cl/NH_4OH. The separated solid

was extracted with chloroform:MeOH (3:1) and filtered through a pad of Celite. The organic layer was washed once with saturated NaCl and dried over anhydrous $MgSO_4$. It was filtered and concentrated. The brown solid obtained was taken to next step without purification: yield 3.8 g, 93%; mp 131 °C; MS $(M + H)^+$ 205.

Step 3: 2-Formylimidazo[2,1-*b*]benzthiazole (20a). To a stirred solution of imidazo[2,1-*b*]benzthiazole-2-methanol (2.04 g, 10 mmol) in chloroform (200 mL) was added activated MnO_2 (15 g, excess). The reaction mixture was refluxed for 24 h and filtered through a pad of Celite. The reaction mixture was concentrated and the product was purified by silica gel column chromatography by eluting it with 75% ethyl acetate: hexane: brown solid; yield 800 mg, 40%; ^{1}H NMR ($CDCl_3$) δ 9.97 (s, 1H), 8.61 (s, 1H), 7.61 (m, 1H), 7.57 (m, 1H), 7.31−7.13 (m, 2H); MS $(M + H)^+$ 203.

Step 4: 4-Nitrobenzyl 6-[(Acetyloxy)(imidazo[2,1-*b*][1,3]-benzothiazol-2-yl)methyl]-6-bromo-7-oxo-4-thia-1-azabicyclo[3.2.0]hept-2-ene-2-carboxylate (10a). To a stirred solution of 2-formylimidazo[2,1-*b*]benzthiazole (**20a**) (444 mg, 2.2 mmol) in dry THF−acetonitrile solution (20 mL and 15 mL) was added anhydrous $MgBr_2$:etherate (619 mg, 2.4 mmol) at room temperature. The reaction mixture was stirred for 30 min and cooled to −20 °C followed by the addition of (5*R*,6*S*)-6-bromo-7-oxo-4-thia-1-azabicyclo[3.2.0]hept-2-ene-2-carboxylic acid 4-nitrobenzyl ester (**9**) (772 mg, 2 mmol) and Et_3N (2.0 mL) under an argon atmosphere. The reaction vessel was covered with foil to exclude light and stirred for 16 h at −20 °C. At the end, the reaction mixture was treated with acetic anhydride (1.04 mL) in one portion. The reaction mixture was warmed to 0 °C and stirred for 15 h at that temperature. The mixture was diluted with ethyl acetate and filtered through a pad of Celite. The pad was washed with ethyl acetate and the filtrate was concentrated under reduced pressure. The residue was purified by a silica gel column by eluting it with ethyl acetate:hexane (1:1). Collected fractions were concentrated under reduced pressure, and the mixture of diastereoisomers was taken to the next step: pale yellow amorphous solid; yield 850 mg, 67%; mp 69 °C; MS $(M + H)^+$ 630.

Step 5: (5*R*,6*Z*)-6-(Imidazo[1,2-*b*][1,3]benzothiazol-2-ylmethylene)-7-oxo-4-thia-1-azabicyclo[3.2.0]hept-2-ene-2-carboxylic Acid Sodium Salt (11). 4-Nitrobenzyl-6-[(acetyloxy)-(imidazo[2,1-*b*][1,3]benzothiazol-2-yl)methyl]-6-bromo-7-oxo-4-thia-1-azabicyclo[3.2.0]hept-2-ene-2-carboxylate (**10a**) (500 mg, 0.79 mmol) was dissolved in THF (17 mL) and acetonitrile (34 mL), and freshly activated Zn dust (5.2 g) was added rapidly along with 0.5 M phosphate buffer (pH 6.5, 28 mL). The reaction vessel was covered with foil to exclude light and vigorously stirred for 2 h at room temperature. The reaction mixture was filtered and cooled to 3 °C. The pH of the filtrate was adjusted to 8.5, and the filtrate was washed with ethyl acetate. The ethyl acetate layer was separated and the aqueous layer was concentrated under high vacuum at 35 °C to give a yellow precipitate. The precipitate was dissolved in acetonitrile/water and loaded on a HP-21 reverse phase column. It was eluted with deionized water (2 L) and latter eluted with 10% acetonitrile:water: yellow crystals; yield 105 mg, 35%; mp 233 °C; ^{1}H NMR (DMSO-d_6) δ 6.51 (s, 1H), 6.53 (s, 1H), 7.09 (s, 1H), 7.47 (t, 1H, J = 7.5 Hz), 7.54 (t, 1H, J = 7.5 Hz), 8,06 (t, 1H), 8.62 (s, 1H); MS $(M + H)^+$ 356, $(M + Na)^+$ 378. Anal. ($C_{16}H_8N_3O_3S_2Na$) C, H, N.

Preparation of (5*R*,6*Z*)-6-[(7-Fluoroimidazo[2,1-*b*][1,3]-benzothiazol-2-ylmethylene)-7-oxo-4-thia-1-azabicyclo-[3.2.0]hept-2-ene-2-carboxylic Acid Sodium Salt (12). Step 1: Ethyl 7-fluoroimidazo[2,1-*b*]benzthiazole-2-carboxylate was prepared according to the procedure outlined for compound **11** (step 1). Starting from 6-fluoro-2-aminobenzothiazole (10.0 g, 59.5 m.mol) and ethyl bromopyruvate (17.4 g, 89.2 mmol), 3.0 g (19% yield) of ethyl 7-fluoro-imidazo[2,1-*b*]benzthiazole-2-carboxylate was isolated as a brown semisolid after purifying the reaction mixture using silica gel column chromatography; MS $(M + H)^+$ 265.

Step 2: 7-Fluoroimidazo[2,1-*b*]benzthiazole-2-methanol was prepared starting from ethyl 7-fluoroimidazo[2,1-*b*]-benzthiazole-2-carboxylate (2.64 g, 0.01 mol) and $LiBH_4$ (50 mg) in THF at refluxing temperature for 2 h. The reaction mixture was quenched with ice-cold water and acidified with 10 N HCl. The reaction mixture was stirred for 1 h and neutralized with K_2CO_3. The separated residue was extracted with chloroform:methanol (3:1), dried over anhydrous $MgSO_4$, filtered, and concentrated. The crude reaction mixture was found to be pure and taken to the next step with out any purification: semisolid; yield 1.5 g 68%; MS $(M + H)^+$ 223.

Step 3: 2-Formyl-7-fluoro-imidazo[2,1-*b*]benzthiazole (20b) was prepared according to the procedure outlined for compound **11** (step 3). Starting from 7-fluoroimidazo[2,1-*b*]-benzthiazole-2-methanol (1.5 g 6.7 mmol) and active MnO_2 (12 g, excess), in boiling chlorofom (300 mL) 1.1 g (78% yield) of the aldehyde derivative was isolated as brown solid. The product was purified by silica gel column chromatography by eluting it with 3:1 ethyl acetate:hexane. ^{1}H NMR ($CDCl_3$) δ 9.8 (s, 1H), 9.1 (s, 1H), 8.2 (dd, 1H, J = 4 Hz), 8.0 (dd, 1H, J = 4 Hz), 7.5 (m, 1H); MS $(M + H)^+$ 221.

Step 4: 4-Nitrobenzyl-6-[(acetyloxy)(7-fluoroimidazo-[2,1-*b*][1,3]benzothiazol-2-yl)methyl]-6-bromo-7-oxo-4-thia-1-azabicyclo[3.2.0]hept-2-ene-2-carboxylate (10b) was prepared according to the procedure outlined for the preparation of compound **11** (step 4). Starting from 2-formyl-7-fluoroimidazo[2,1-*b*]benzthiazole (**20b**) (500 mg, 2.3 mmol) and (5*R*,6*S*)-6-bromo-7-oxo-4-thia-1-azabicyclo[3.2.0]hept-2-ene-2-carboxylic acid 4-nitro-benzyl ester (**9**) (875 mg, 2.3 mmol), compound **10b** was isolated as a mixture of diastereoisomers, which were taken to the next step. Prior to that, the compound was purified by silica gel column chromatography by eluting it with 1:1 ethyl acetate:hexane: pale yellow amorphous solid; yield 330 mg, 22%; MS $(M + H)^+$ 649.

Step 5: (5*R*,6*Z*)-6-[(7-Fluoroimidazo[1,2-*b*][1,3]benzothiazol-2-ylmethylene)]-7-oxo-4-thia-1-azabicyclo[3.2.0]-hept-2-ene-2-carboxylic acid sodium salt (12) was prepared according to the procedure outlined for the preparation of compound **11** (step 5). Starting from 4-nitrobenzyl-6-[(acetyloxy)(7-fluoroimidazo[2,1-*b*][1,3]benzothiazol-2-yl)methyl]-6-bromo-7-oxo-4-thia-1-azabicyclo[3.2.0]hept-2-ene-2-carboxylate (**10b**) (710 mg, 1.07 mmol), compound **12** was isolated as a yellow amorphous solid after purification using an HP-21 reverse phase column: yellow crystals; yield 80 mg, 19%; mp 200 °C (dec); ^{1}H NMR (DMSO-d_6) δ 6.53 (s, 1H), 6.63 (s, 1H), 7.1 (s, 1H), 7.45 (t, 1H), 8.04 (m, 1H), 8,13−8.10 (m, 1H), 8.61 (s, 1H); MS $(M + Na)^+$ 396. Anal. ($C_{16}H_7FN_3O_3S_2Na$) C, H, N.

Preparation of (5*R*,6*Z*)-6-[(7-Chloroimidazo[2,1-*b*][1,3]-benzothiazol-2-ylmethylene)-7-oxo-4-thia-1-azabicyclo-[3.2.0]hept-2-ene-2-carboxylic Acid Sodium Salt (13). Step 1: Ethyl 7-chloroimidazo[2,1-*b*]benzthiazole-2-carboxylate was prepared according to the procedure outlined for the preparation of compound **11** (step 1). Starting from 6-chloro-2-aminobenzothiazole (9.2 g, 50 mmol) and ethyl bromopyruvate (11.6 g, 60 mmol), 8.5 g (60% yield) of ethyl 7-chloroimidazo[2,1-*b*]benzthiazole-2-carboxylate was isolated as a brown solid. The product was purified using silica gel column chromatography by eluting with 1:1 ethyl acetate: hexane; MS $(M + H)^+$ 281.

Step 2: 7-Chloroimidazo[2,1-*b*]benzthiazole-2-methanol was prepared according to the procedure outlined for the preparation of compound **11** (step 2). Starting from ethyl 7-chloroimidazo[2,1-*b*]benzthiazole-2-carboxylate (9.0 g, 32.1 mmol) and $LiAlH_4$ (4.0 g, excess), 5.5 g (72% yield) of the alcohol derivative was isolated as a brown solid. The product was found to be pure enough and taken to the next step without purification: mp 166 °C; MS $(M + H)^+$ 239.

Step 3: 2-Formyl-7-chloroimidazo[2,1-*b*]benzthiazole (20c) was prepared according to the procedure outlined for the preparation of compound **11** (step 3). Starting from 7-chloroimidazo[2,1-*b*]benzthiazole-2-methanol (4.0 g 16.8 mmol) in refluxing chloroform:methanol (300:50 mL) and active MnO_2 (20 g, excess), 2.2 g (55% yield) of the aldehyde derivative was isolated as a brown solid. Product was purified by silica gel column chromatography by eluting it with 1:1 ethyl acetate:

hexane: ^{1}H NMR ($CDCl_3$) δ 9.9 (s, 1H), 8.3 (s, 1H), 7.7 (s, 1H), 7.6 (d, 1H, J = 8 Hz), 7.5 (m, 1H); MS $(M + H)^+$ 236.

Step 4: 4-Nitrobenzyl-6-[(acetyloxy)(7-chloroimidazo-[2,1-*b*][1,3]benzothiazol-2-yl)methyl]-6-bromo-7-oxo-4-thia-1-azabicyclo[3.2.0]hept-2-ene-2-carboxylate (10c) was prepared according to the procedure outlined for the preparation of compound **11** (step 4). Starting from 2-formyl-7-chloroimidazo[2,1-*b*]benzthiazole (**20c**) (270 mg, 1.14 mmol) and (5*R*,6*S*)-6-bromo-7-oxo-4-thia-1-azabicyclo[3.2.0]hept-2-ene-2-carboxylic acid 4-nitrobenzyl ester (**9**) (500 mg, 1.14 mmol), compound **10c** was isolated as a mixture of diastereoisomers, which were taken to the next step. Prior to that, the compound was purified by silica gel column chromatography by eluting with 1:1 ethyl acetate:hexane: pale yellow amorphous solid; yield 495 mg, 65%; MS $(M + H)^+$ 665.

Step 5: (5*R*,6*Z*)-6-[(7-Chloroimidazo[1,2-*b*][1,3]benzothiazol-2-ylmethylene)]-7-oxo-4-thia-1-azabicyclo[3.2.0]-hept-2-ene-2-carboxylic acid sodium salt (13) was prepared according to the procedure outlined for the preparation of compound **11** (step 5). Starting from 4-nitrobenzyl-6-[(acetyloxy)(7-chloroimidazo[2,1-*b*][1,3]benzothiazol-2-yl)methyl]-6-bromo-7-oxo-4-thia-1-azabicyclo[3.2.0]hept-2-ene-2-carboxylate (**10c**), compound **13** was isolated as a yellow amorphous solid after purification using an HP-21 reverse phase column. The yellow solid was washed with acetone, filtered, and dried: yellow crystals; yield 80 mg, 18%; mp 240 °C; ^{1}H NMR (DMSO-d_6) δ 6.6 (s, 2H), 7.1 (s, 1H), 7.62 (dd, 1H), 8.11 (d, 1H), 8.2 (s, 1H), 8.6 (s, 1H); MS $(M + H + Na)^+$ 412. Anal. ($C_{16}H_7ClN_3O_3S_2Na$) C, H, N.

Preparation of (5*R*,6*Z*)-6-[(7-methylimidazo[2,1-*b*][1,3]-benzothiazol-2-ylmethylene)-7-oxo-4-thia-1-azabicyclo-[3.2.0]hept-2-ene-2-carboxylic Acid Sodium Salt (14). Step 1: Ethyl 7-methylimidazo[2,1-*b*]benzthiazole-2-carboxylate was prepared according to the procedure outlined for the preparation of compound **11** (step 1). Starting from 6-methyl-2-aminobenzothiazole (3.2 g, 20 mmol) and ethyl bromopyruvate (4.0 g, 20.4 mmol), 3.0 g (57% yield) of ethyl 7-methylimidazo[2,1-*b*]benzthiazole-2-carboxylate was isolated as a brown solid. The product was purified by silica gel column chromatography by eluting with 1:1 ethyl acetate:hexane: MS $(M + H)^+$ 261.

Step 2: 2-Formyl-7-methylimidazo[2,1-*b*]benzthiazole (20d). To a stirred solution of ethyl 7-methylimidazo[2,1-*b*]-benzthiazole-2-carboxylate (4.0 g, 15.38 mmol) in dry THF at −78 °C was added DIBAL (1 M solution in toluene) (16.0 mL, 16 mmol). The reaction mixture was stirred at −78 °C and slowly elevated to room temperature. The reaction mixture was stirred at room temperature for 30 min and quenched with saturated NH_4Cl. The reaction mixture was extracted with chloroform and washed well with water. The organic layer was dried over anhydrous $MgSO_4$, filtered, and concentrated. The residue was purified by SiO_2 column chromatography by eluting with chloroform:methanol (20:1): brown solid; yield 800 mg, 24%; ^{1}H NMR ($CDCl_3$) δ 9.3 (s, 1H), 8.3 (s, 1H), 7.6−7.5 (m, 2H), 7.36 (s, 1H), 2.4 (s, 3H); MS $(M + H)^+$ 217.

Step 3: 4-Nitrobenzyl 6-[(acetyloxy) (7-methylimidazo-[2,1-*b*][1,3]benzothiazol-2-yl)methyl]-6-bromo-7-oxo-4-thia-1-azabicyclo[3.2.0]hept-2-ene-2-carboxylate (10d) was prepared according to the procedure outlined for the preparation of compound **11** (step 4). Starting from 2-formyl-7-methylimidazo[2,1-*b*]benzthiazole (**20d**) (432 mg, 2.0 mmol) and (5*R*,6*S*)-6-bromo-7-oxo-4-thia-1-azabicyclo[3.2.0]hept-2-ene-2-carboxylic acid 4-nitro-benzyl ester (**9**) (772 mg, 2.0 mmol), compound **10d** was isolated as a mixture of diastereoisomers, which were taken to the next step. Prior to that, the compound was purified by silica gel column chromatography by eluting with 1:1 ethyl acetate:hexane: pale yellow amorphous solid; yield 400 mg, 31%; MS $(M + H)^+$ 645.

Step 4: (5*R*,6*Z*)-6-[(7-Methylimidazo[1,2-*b*][1,3]benzothiazol-2-ylmethylene)]-7-oxo-4-thia-1-azabicyclo[3.2.0]-hept-2-ene-2-carboxylic acid sodium salt (14) was prepared according to the procedure outlined for the preparation of compound **11** (step 5). Starting from 4-nitrobenzyl 6-[(acetyloxy)(7-methylimidazo[2,1-*b*][1,3]benzothiazol-2-yl)methyl]-6-bromo-7-oxo-4-thia-1-azabicyclo[3.2.0]hept-2-ene-2-carboxylate (**10d**) (350 mg, 0.54 mmol) compound **14** was isolated as yellow amorphous solid after the purification using an HP-21 reverse phase column. The yellow solid was washed with acetone, filtered, and dried: yellow crystals; yield 110 mg, 55%; mp 178 °C (dec); ^{1}H NMR (DMSO-d_6) δ 8.56 (s, 1H), 7.93 (d, 1H), 7.83 (s, 1H), 7.38 (d, 1H), 7.07 (s, 1H), 6.51 (s, 2H), 2.42 (s, 3H); MS $(M + H + Na)^+$ 392. Anal. ($C_{17}H_{10}N_3O_3S_2Na$) C, H, N.

Step 4: (5*R*,6*Z*)-6-[(7-Methylimidazo[1,2-*b*][1,3]benzothiazol-2-ylmethylene)]-7-oxo-4-thia-1-azabicyclo [3.2.0]-hept-2-ene-2-carboxylic Acid Sodium Salt (14) (Procedure B). 4-Nitrobenzyl 6-[(acetyloxy)(7-methylimidazo[2,1-*b*]-[1,3]benzothiazol-2-yl)methyl]-6-bromo-7-oxo-4-thia-1-azabicyclo-[3.2.0]hept-2-ene-2-carboxylate (350 mg, 0.54 mmol) was dissolved in THF (40 mL) and 6.5 pH phosphate buffer (40 mL) and hydrogenated over Pd/C (10%, 200 mg) at 40 psi pressure for 3 h at room temperature. The reaction mixture was filtered through a pad of Celite and washed with acetonitrile. The reaction mixture was concentrated to 40 mL and cooled to 0 °C, and the pH was adjusted to 8.5 by adding 1 N NaOH. The product was directly loaded over an HP21 resin reverse phase column. Initially, the column was eluted with deionized water (2 L) and later with 10% acetonitrile:water. The fractions were concentrated and the yellow solid was washed with acetone, filtered, and dried: yield 110 mg, 55%.

Preparation of (5*R*,6*Z*)-6-[(7-Methoxyimidazo[2,1-*b*][1,3]-benzothiazol-2-ylmethylene)-7-oxo-4-thia-1-azabicyclo[3.2.0]-hept-2-ene-2-carboxylic Acid Sodium Salt (15). Step 1: Ethyl 7-methoxyimidazo[2,1-*b*]benzthiazole-2-carboxylate was prepared according to the procedure outlined for compound **11** (step 1). Starting from 6-methoxy-2-amino benzothiazole (27 g, 0.15 mol) and ethyl bromopyruvate (39.9 g, 0.2 mol), 24 g (43% yield) of ethyl 7-methoxyimidazo[2,1-*b*]-benzthiazole-2-carboxylate was isolated as a brown solid. The product was purified by silica gel column chromatography by eluting with 1:1 ethyl acetate:hexane: MS $(M + H)^+$ 277.

Step 2: 7-Methoxyimidazo[2,1-*b*]benzthiazole-2-methanol was prepared according to the procedure outlined for compound **11** (step 2). Starting from ethyl 7-methoxyimidazo-[2,1-*b*]benzthiazole-2-carboxylate (12.5 g, 43.5 mmol) and $LiAlH_4$ solution (43.5 mL, 0.5 M solution in THF), 4.0 g (40% yield) of the alcohol derivative was isolated as a brown solid: MS $(M + H)^+$ 235.

Step 3: 2-Formyl-7-methoxyimidazo[2,1-*b*]benzthiazole (20e) was prepared according to the procedure outlined for compound **11** (step 4). Starting from 7-methoxyimidazo-[2,1-*b*]benzthiazole-2-methanol (4.0 g 17 mmol) in refluxing chloroform (300 mL) and active MnO_2 (12 g, excess), 822 mg (21% yield) of the aldehyde derivative was isolated as brown solid: ^{1}H NMR ($CDCl_3$) δ 9.9 (s, 1H), 8.3 (s, 1H), 7.6 (d, 1H, J = 9 Hz), 7.24 (d, 1H, J = 2.4 Hz), 7.05 (m, 1H), 3.9 (s, 3H); MS $(M + H)^+$ 233.

Step 4: 4-Nitrobenzyl 6-[(acetyloxy)(7-methoxyimidazo[2,1-*b*][1,3]benzothiazol-2-yl)methyl]-6-bromo-7-oxo-4-thia-1-azabicyclo[3.2.0]hept-2-ene-2-carboxylate (10e) was prepared according to the procedure outlined for the preparation of compound **11** (step 4). Starting from 2-formyl-7-methoxyimidazo[2,1-*b*]benzthiazole (**20e**) (822 mg, 3.5 mmol) and (5*R*,6*S*)-6-bromo-7-oxo-4-thia-1-aza-bicyclo[3.2.0]hept-2-ene-2-carboxylic acid 4-nitrobenzyl ester (**9**) (1.364, 3.54 mmol), compound **10e** was isolated as a mixture of diastereoisomers, which were taken to next step. Prior to that, the compound was purified by silica gel column chromatography by eluting with 1:1 ethyl acetate:hexane: pale yellow amorphous solid; yield 2.24 g, 95%; MS $(M + H)^+$ 660.

Step 5: (5*R*,6*Z*)-6-[(7-methoxyimidazo[1,2-*b*][1,3]benzothiazol-2-ylmethylene)]-7-oxo-4-thia-1-azabicyclo[3.2.0]-hept-2-ene-2-carboxylic acid sodium salt (15) was prepared according to the procedure outlined for the preparation of compound **11** (step 5). Starting from 4-nitrobenzyl-6-[(acetyloxy)(7-methoxyimidazo[2,1-*b*][1,3]benzothiazol-2-yl)methyl]-6-bromo-7-oxo-4-thia-1-azabicyclo[3.2.0]hept-2-ene-2-carboxylate (**10e**)

(659 mg, 1.0 mmol), compound **15** was isolated as a yellow amorphous solid after purification using an HP-21 reverse phase column. The precipitate was filtered and washed with H_2O, MeCN, and acetone to give the title compound: yellow crystals; yield: 68 mg, 23%; mp 284 °C; ^{1}H NMR (DMSO-d_6) δ 3.89 (s, 3H), 6.58 (s, 1H), 6.64 (s, 1H), 7.14 (s, 1H), 7.2 (dd, 1H, J = 6.0 Hz), 7.75 (d, 1H, J = 3.0 Hz), 8.03 (d, J = 6.0 Hz, 1H), 8.62 (s, 1H); MS (M + H)$^+$ 386, (M + Na)$^+$ 407. Anal. ($C_{17}H_{10}N_3O_4S_2Na$) C, H, N.

Preparation of (5*R*,6*Z*)-6-[(5-Methylimidazo[2,1-*b*][1,3]-benzothiazol-2-ylmethylene)-7-oxo-4-thia-1-azabicyclo-[3.2.0]hept-2-ene-2-carboxylic acid sodium salt (16). Step 1: Ethyl 5-methylimidazo[2,1-*b*]benzthiazole-2-carboxylate was prepared according to the procedure outlined for compound **11** (step 1). Starting from 4-methyl-2-aminobenzothiazole (8.0 g, 48.7 mmol) and ethyl bromopyruvate (14.0 g, 71.7 mmol), 6.0 g (45% yield) of ethyl 5-methylimidazo[2,1-*b*]benzthiazole-2-carboxylate was isolated as a brown solid. The product was purified by silica gel column chromatography by eluting it with 1:1 ethyl acetate:hexane. MS (M + H)$^+$ 261.

Step 2: 5-Methylimidazo[2,1-*b*]benzthiazole-2-methanol was prepared according to the procedure outlined for the preparation of compound **11** (step 2). Starting from ethyl 5-methylimidazo[2,1-*b*]benzthiazole-2-carboxylate (5.2 g, 20 mmol) and $LiAlH_4$ solution (22 mL, 0.5 M solution in THF), 3 g (69% yield) of the alcohol derivative was isolated as a brown solid; MS (M + H)$^+$ 219.

Step 3: 2-Formyl-5-methylimidazo[2,1-*b*]benzthiazole (20f) was prepared according to the procedure outlined for the preparation of compound **11** (step 3), starting from 5-methylimidazo[2,1-*b*]benzthiazole-2-methanol (2.0 g, 9.1 mmol) in refluxing chloroform:methanol (300:50 mL) and active MnO_2 (12 g, excess): brown solid; yield 700 mg 35%; ^{1}H NMR ($CDCl_3$) δ 9.9 (s, 1H), 8.5 (s, 1H), 7.5 (d, 1H, J = 8 Hz), 7.3−7.1 (m, 2H), 2.7 (s, 3H); MS (M + H)$^+$ 217.

Step 4: 4-Nitrobenzyl 6-[(acetyloxy) (5-methylimidazo-[2,1-*b*][1,3]benzothiazol-2-yl)methyl]-6-bromo-7-oxo-4-thia-1-azabicyclo[3.2.0]hept-2-ene-2-carboxylate (10f) was prepared according to the procedure outlined for the preparation of compound **11** (step 4). Starting from 2-formyl-5-methylimidazo[2,1-*b*]benzthiazole (**20f**) (432 mg, 2.0 mmol) and (5*R*,6*S*)-6-bromo-7-oxo-4-thia-1-aza-bicyclo[3.2.0]hept-2-ene-2-carboxylic acid 4-nitrobenzyl ester (**9**) (770 mg, 2 mmol), compound **10f** was isolated as a mixture of diastereoisomers, which were taken to the next step. Prior to that, compound was purified by silica gel column chromatography by eluting with 1:1 ethyl acetate:hexane: pale yellow amorphous solid; yield 270 mg, 20%; MS (M + H)$^+$ 644.

Step 5: (5*R*,6*Z*)-6-[(5-Methylimidazo[1,2-*b*][1,3]benzothiazol-2-ylmethylene)]-7-oxo-4-thia-1-azabicyclo[3.2.0]-hept-2-ene-2-carboxylic acid sodium salt (16) was prepared according to the procedure outlined for the preparation of compound **11** (step 5). Starting from 4-nitrobenzyl-6-[(acetyloxy)(5-methylimidazo[2,1-*b*][1,3]benzothiazol-2-yl)-methyl]-6-bromo-7-oxo-4-thia-1-azabicyclo[3.2.0]hept-2-ene-2-carboxylate (**10f**) (400 mg, 0.62 mmol) compound **16** was isolated as yellow an amorphous solid after purification using an HP-21 reverse phase column. The precipitate was filtered and washed with H_2O, MeCN, and acetone to give the title compound: yellow crystals; yield 60 mg, 24%; mp 192 °C; ^{1}H NMR (DMSO-d_6) δ 2.1 (s, 3H), 6.53 (s, 2H), 7.1 (s, 1H), 7.34−7.36 (m, 2H), 7.85 (m, 1H), 8.58 (s, 1H); MS (M + Na)$^+$ 392. Anal. ($C_{17}H_{10}N_3O_3S_2Na$) C, H, N.

Preparation of (5*R*,6*Z*)-6-(6,7-Dihydro-5*H*-cyclopenta-[*d*]imidazo[2,1-*b*][1,3]thiazol-2-ylmethylene)-7-oxo-4-thia-1-azabicyclo[3.2.0]hept-2-ene-2-carboxylic Acid Sodium Salt (17). Step 1: Preparation of Ethyl 6,7-Dihydro-5*H*-cyclopenta[*d*]imidazo[2,1-*b*][1,3]thiazole-2-carboxylate. A mixture of 2-chlorocyclopentanone (11.8 g, 100 mmol) and thiourea (8.0 g 101 mmol) was refluxed in ethanol:THF (1:2) for 16 h. The reaction mixture was cooled to room temperature and the separated white solid was filtered (9.0 g separated). This was dissolved in anhydrous ethanol (100 mL) and sodium methoxide (2.7 g, 51 mmol). To this was added ethyl bromopyruvate (10 0.0 g) and the mixture stirred at room temperature for 2 h. Then it was refluxed for 48 h. The reaction mixture was cooled to room temperature and concentrated. The residue was extracted with chloroform and washed well with water. The product was purified by silica gel column chromatography by eluting with 50% ethyl acetate:hexane: red semisolid; yield 3.0 g 13%; MS (M + H)$^+$ 237.

Step 2: 6,7-Dihydro-5*H*-cyclopenta[*d*]imidazo[2,1-*b*]-[1,3]thiazole-2-methanol was prepared according to the procedure outlined for the preparation of compound **11** (step 2). Starting from ethyl 6,7-dihydro-5*H*-cyclopenta[*d*]imidazo-[2,1-*b*][1,3]thiazole-2-carboxylate (4.7 g, 20 mmol) and $LiAlH_4$ solution (22 mL, 0.5 M solution in THF), 2.5 g (62% yield) of the alcohol derivative was isolated as a brown solid; MS (M + H)$^+$ 195.

Step 3: 2-Formyl-6,7-dihydro-5*H*-cyclopenta[d]imidazo-[2,1-*b*][1,3]thiazole (24) was prepared according to the procedure outlined for the preparation of compound **11** (step 3). Starting from 6,7-dihydro-5*H*-cyclopenta[*d*]imidazo[2,1-*b*]-[1,3]thiazole-2-methanol (2.0 g, 10.3 mmol) in refluxing chloroform:methanol (300:50 mL) and active excess MnO_2 (12 g,), 900 mg (45%) of the aldehyde derivative was isolated as a brown solid. ^{1}H NMR ($CDCl_3$) δ 9.9 (s, 1H), 7.9 (s, 1H), 2.97−2.95 (m, 4H), 2.59−2.55 (m, 2H); MS (M + H)$^+$ 193.

Step 4: 4-Nitrobenzyl (5*R*)-6-[(acetyloxy)(6,7-dihydro-5*H*-cyclopenta[*d*]imidazo[2,1-*b*][1,3]thiazol-2-yl)-6-bromo-7-oxo-4-thia-1-azabicyclo[3.2.0]hept-2-ene-2-carboxylate (10g) was prepared according to the procedure outlined for the preparation of compound **11** (step 4). Starting from 2-formyl-6,7-dihydro-5*H*-cyclopenta[*d*]imidazo[2,1-*b*][1,3]-thiazole (**24**) (600 mg, 3.1 mmol) and (5*R*,6*S*)-6-bromo-7-oxo-4-thia-1-azabicyclo[3.2.0]hept-2-ene-2-carboxylic acid 4-nitrobenzyl ester (**9**) (1.2 g, 3 mmol), compound **10g** was isolated as a mixture of diastereoisomers, which were taken to the next step. Prior to that, the compound was purified by silica gel column chromatography by eluting with 1:1 ethyl acetate: hexane: pale yellow amorphous solid; yield 850 mg, 45%; MS (M + H)$^+$ 620.

Step 5: (5*R*,6*Z*)-6-(6,7-Dihydro-5H-cyclopenta[*d*]imidazo[2,1-*b*][1,3]thiazol-2-ylmethylene)-7-oxo-4-thia-1-azabicyclo[3.2.0]hept-2-ene-2-carboxylic acid sodium salt (17) was prepared according to the procedure outlined for the preparation of compound **11** (step 5). Starting from 4-nitrobenzyl (5*R*)-6-[(acetyloxy)(6,7-dihydro-5*H*-cyclopenta[*d*]imidazo-[2,1-*b*][1,3]thiazol-2-yl)-6-bromo-7-oxo-4-thia-1-azabicyclo[3.2.0]-hept-2-ene-2-carboxylate (850 mg, 1.37 mmol), compound **17** was isolated as a yellow amorphous solid after purification using an HP-21 reverse phase column. The yellow solid was washed with acetone, filtered, and dried: yellow crystals; yield 138 mg, 29%; mp 192°C; ^{1}H NMR (DMSO-d_6) δ 2.51 (m, 4H), 3.01 (m, 2H), 8.2 (s, 1H), 7.1 (s, 1H), 6.55 (s, 1H), 6.4 (s, 1H); MS (M + H + Na)$^+$ 367. Anal. ($C_{15}H_{10}N_3O_3S_2Na$) C, H, N.

Acknowledgment. X-ray data for the SHV-1 complex were collected at the Institute of Materials Science of the University of Connecticut. Data for GC1 were obtained at the Cornell High Energy Synchrotron Source (CHESS, supported by NSF Award DMR-9311772), using the Macromolecular Diffraction facility (MacCHESS, supported by NIH Award RR-01646). Work in Cleveland was supported by a Department of Veterans Affairs Merit Review Award to R.A.B. The authors thank the members of Wyeth's Chemical Technology Department for analytical and spectral determination and Drs. David Shlaes and Beth Rasmussen for stimulating discussions and encouragement.

Appendix

Abbreviations. Cymal-6, cyclohexyl-(*n*-hexyl)-β-D-maltoside; HEPES, *N*-(2-hydroxyethyl)piperazine-*N*′-(2-ethanesulfonic acid); IC_{50}, concentration of a drug that

will result in 50% inhibition of the target enzyme; LDA, lithium diisopropylamide; LiHMDS, lithium hexamethyldisilazide; MIC, concentration of the lowest dilution of the drug in which bacterial growth is absent as detected by the unaided eye; MPD, 2-methyl-2,4-pentanediol; PEG, poly(ethyleneglycol); rmsd, root-mean-square deviation.

Supporting Information Available: Crystallographic refinement data (Table 1), X-ray data collection (Table 2), and elemental analysis data for compounds **11**−**17**. This material is available free of charge via the Internet at http://pubs.acs.org.

References

(1) (a) Sandanayaka, V. P.; Prashad, A. S. Resistance to β-Lactam Antibiotics: Structure and Mechanism Based Drug Design of β-Lactamase Inhibitors. *Curr. Med. Chem.* **2002**, *9*, 1145−1165, (b) Micetich, R. G.; Salama, S. M.; Maiti, S. N.; Reddy, A. V. N.; Singh, R. β-Lactamases and Their Inhibitors: An Update. *Curr. Med. Chem: Anti-infect Agents.* **2002**, *1*, 193-213. (c) Bradford, P. A. Extended Spectrum β-Lactamases in the 21st Century: Characterization, Epidemiology and Detection of This Important Resistance Threat. *Clin. Microbiol. Rev.* **2001**, *4*, 933−951. (d) Bradford, P. A. What is New in β-Lactamases? *Curr. Inf. Dis. Rep.* **2001**, *3*, 13−19. (e) Bush, K. β-Lactamases of Increasing Clinical Importance. *Curr. Pharm. Design* **1999**, *5*, 839−845. (f) Payne, D. J.; Wensheng, D.; Bateson, J. H. β−Lactamase Epidemiology and the Utility of Established and Novel β−Lactamase Inhibitors. *Expert Opin. Invest. Drugs* **2000**, *9*, 247−261. (g) Knox, J. R. Extended-Spectrum and Inhibitor-Resistant TEM-Type β-Lactamases: Mutations, Specificity and Three-Dimensional Structure. *Antimicrob. Agents Chemother.* **1995**, *39*, 2593−2601. (h) Yang, Y.; Rasmussen, B. A.; Shlaes, D. M. Class A β-Lactamases−Enzyme−Inhibitor Interactions and Resistance. *Pharmacol. Therapeutics* **1999**, *83,* 141−151 (i) Bonnefoy, A.; Dupuis-Hamelin, C.; Steier, V.; Delachaume, C.; Seys, C.; Stachyra, T.; Fairley, M.; Guitton, M.; Lampilas, M. In Vitro Activity of AVE1330A, an Innovative Broad-Spectrum Non-β-Lactam β-Lactamase Inhibitor. *J. Antimicrob. Chemother*. **2004**, *54*, 410−417.

(2) Jones, C. H.; Hruby, D. E. New Targets for Antibiotic Development: Biogenesis of Surface Adherence Structures. *Drug Discovery Today* **1998**, *3*, 495−504.

(3) (a) Bennett, I. S.; Broom, N. J. P.; Bruton, G.; Calvert, S. A.; Clarke, B. P.; Coleman, K.; Edmondson, R.; Edwards, P.; Jones, D.; Osborne, N. F.; Walker, G. 6-(Substituted Methylene) Penems: Potent Broad Spectrum Inhibitors of Bacterial β-Lactamase III. Structure−Activity Relationships of the five-membered Heterocyclic Derivatives. *J. Antibiotics* **1991**, *44*, 331−343. (b) Bennett, I. S.; Brooks, G.; Brown, N. J. P.; Calvert, S. H.; Coleman, K.; Francois, I. 6-(Substituted Methylene) Penems: Potent Broad Spectrum Inhibitors of Bacterial β-Lactamase V. Chiral 1,2,3-Triazolyl Derivatives. *J. Antibiotics* **1991**, *44*, 969−978.

(4) Bulychev, A.; Massova, I.; Lerner, S. A.; Mobashery, S. Penem BRL 42715: An Effective Inactivator for β-Lactamases. *J. Am. Chem. Soc.* **1995**, *117*, 4797−4801.

(5) Broom, N. J. P.; Farmer, T. H.; Osborne, N. F.; Tyler, J. W. Studies on the Mechanism of Action of 5R-Z-6-(1-Methyl-1,2,3-Triazol-4-ylmethylene)Penem-3-Carboxylic Acid (BRL 42715), a Potent Inhibitor of Bacterial β-Lactamase. *J. Chem. Soc. Chem. Commun.* **1992**, 1663−1664.

(6) Chen, L. Y.; Chang, C.-W.; Hedberg, K.; Guarineo, K.; Welch, W. M.; Kiessling, L.; Retsema, J. A.; Haskell, S. L.; Anderson, M.; Manousos, M.; Barrett, J. F. Structure−Activity Relationships of 6-(Hetereocyclyl)-Methylene Penam Sulfones, a New Class of β-Lactamase Inhibitors. *J. Antibiotics* **1987**, *40*, 803−822.

(7) Buynak, J. D.; Wu, K.; Bachmann, B.; Khasnis, D.; Hua, L.; Wguyen, H. K.; Carver, C. L. Synthesis and Biological Activity of 7-Alkylidenecephems. *J. Med. Chem.* **1995**, *38*, 1022−1034.

(8) Philips, O. A.; Czajkowski, D. P.; Spevak, P.; Singh, M. P.; Hanehara-Kunugita, C.; Hyodo, A.; Micetich, R. G.; Maiti, S. N. Syn-1012: A New β-Lactamase Inhibitor of Penem Skeleton. *J. Antibiotics* **1997**, *50*, 350−356.

(9) (a) Sandanayaka, V. P.; Yang, Y. Dipolar Cycloaddition of Novel 6-(Nitrileoxidomethyl) penam sulfone: An Efficient Route to a New Class of β-Lactamase Inhibitors. *Org. Lett.* **2000**, *2*, 3087−3090. (b) Sandanayaka, V. P. Allyl and Propargyl Substituted Penam Sulfones as Versatile Intermediates Toward the Synthesis of New β-Lactamase Inhibitors. *Bioorg. Med. Chem. Lett.* **2001**, *11*, 997−1000. (c) Bitha, P.; Zhong, L.; Francisco, G. D.; Rasmussen, B.; Lin, Y. I. 6-(1-Hydroxyalkyl) Penam Sulfone Derivatives as Inhibitors of Class-A and Class-C β-Lactamase I. *Bioorg. Med. Chem. Lett.* **1999**, *9*, 991−996. (d) Bitha, P.; Zhong, L.; Francisco, G. D.; Yang, Y.; Petersen, P. J. B.; Lin, Y. I. 6-(1-Hydroxalkyl) Penam Sulfone Derivatives as Inhibitors of Class-A and Class-C β-Lactamase II. *Bioorg. Med. Chem. Lett.* **1999**, *9*, 997−1002.

(10) Sandanayaka, V. P.; Prashad, A. S.; Yang, Y.; Williamson, T.; Lin, Y. I.; Mansour, T. S. Spirocyclopropyl β-Lactams as Mechanism Based Inhibitors of Serine β-Lactamases. Synthesis by Rhodium-Catalyzed Cyclopropanation of 6-Diazo Penicillanate Sulfones. *J. Med. Chem.* **2003**, *46*, 2569−2571.

(11) (a) Abe, T.; Ushirogochi, H.; Yamamura, I.; Kumagai, T.; Mansour, T. S.; Venkatesan, A. M.; Agarwal, A.; Petersen, P. J.; Weiss, W. J.; Lenoy, E.; Yang, Y.; Shlaes, D. Novel Penem Bearing a Methylidene Linkage as a Broad Spectrum β-Lactamase Inhibitors. Poster presented at 43rd ICCAC, Chicago, IL, 2003, no. 538. (b) Tabei, K.; Feng, X.; Venkatesan, A. M.; Abe, T.; Hideki, U.; Mansour, T. S.; Siegel, M. M., Mechanism of Inactivation of β-Lactamases by Novel 6-Methylidene Penems Elucidated Using Electrospray Ionization Mass Spectrometry. *J. Med. Chem*. **2004**, *47*, 3674−3688.

(12) Nukaga, M.; Abe, T.; Venkatesan, A. M.; Mansour, T. S.; Bonomo, R. A.; Knox, J. R. Inhibition of Class-A and Class-C β-Lactamases by Penems: Crystallographic Structures of Novel 1,4-Thiazepine Intermediate. *Biochemistry* **2003**, *42*, 13152−13159.

(13) Abe, T.; Matsunaga, H.; Mihira, A.; Sato, C.; Ushirogochi, H.; Takasaki, T.; Venkatesan, A. M.; Mansour, T. S. Preparation of Heteroaryl-6-alkylidene-penems as β-Lactamase Inhibitors for Use as Antibacterial Agents, 2003, WO-2003093277.

(14) (a) Osborne, N. F.; Atkins, R. J.; Broom, N. J. P.; Coulton, S.; Harbridge, J. B.; Harris, M. A.; Francois, I. S.; Walker, Synthesis of (5*R*)-(*Z*)-6-(1-Methyl-1,2,3-triazol-4-ylmethylene) Penem-3-carboxylic Acid, a Potent Broad Spectrum β-Lactamase Inhibitor, from 6-Aminopenicillanic Acid G. *J. Chem. Soc Perkin Trans. 1*. **1994**, 179−188. (b) Bennett, I.; Broom, N. J.; Bruton, G.; Calvert, S.; Clarke, G. P.; Coleman, K.; Edmondson, R.; Edwarda, P.; Jones, D.; Osborne, N. F.; 6-(Substituted Methylene)-Penems Potent Boad Spectrum Inhibitors of Bacterial Beta-Lactamases. III Structure−Activity Relationships of the Five-Membered Heterocyclic Derivatives. *J. Antibiotics* **1991**, 44, 331−337.

(15) (a) Bouffard, C. F. A.; Christensen, B. G. Thienamycin Total Synthesis: Introduction of the Hydroxyethyl Side Chain *J. Org. Chem.* **1981**, *46*, 2208−2212. (b) Dininno, F.; Beatte, T. R.; Christensen, B. G. Aldol Condensation of Regiospecific Penicillanate and Cephalosporonate Enolates. Hydroxyethylation at C6 and C7. *J. Org. Chem.* **1977**, *42*, 2960−2965.

(16) Brunger, A. T., Adams, P. D.; Clove, G. M.; Delano, W. L.; Gros, P.; Gross Kunstleve, R. W.; Jiang, J.-S.; Kuszewski, J.; Nilges, M.; Pannu, N. S.; Read, R. J.; Rice, L. M.; Simonson, T.; Warren, G. L. CNS (Crystallography and NMR System). *Acta Crystallogr.* **1998**, *D54*, 905−921.

(17) Brunger, A. T. The Free R Value: A Novel Statistical Quantity for Assessing the Accuracy of Crystal Structures. *Nature* **1992**, *355*, 472−475.

(18) McRee, D. E. XtalView/Xfit−A Versatile Program for Manipulating Atomic Coordinates and Electron Density. *J. Struct. Biol.* **1992**, *125*, 156−165.

(19) Sheldrick, G. M.; Schneider, T. R. SHELX: High-Resolution Refinement. *Methods Enzymol.* **1997**, *277*, 319−343.

(20) Kuzin, A. P.; Nukaga, M.; Nukaga, Y.; Hujer, A. M.; Bonomo, R. A.; Knox, J. R. Structure of the SHV-1 β-Lactamase. *Biochemistry* **1999**, *38*, 5720−5727.

(21) Crichlow, G. V.; Kuzin, A. P.; Nukaga, M.; Sawai, T.; Knox, J. R. Structure of the Extended-Spectrum Class C β-Lactamase of *Enterobacter cloacae* GC1, a Natural Mutant with a Tandem Tripeptde Insertion. *Biochemistry* **1999**, *38*, 10256−10261.

(22) Crichlow, G. V.; Nukaga, M., Doppalapudi, V. R.; Buynak, J. D.; Knox, J. R. Inhibition of Class C β-Lactamases: Structure of a Reaction Intermediate with a Cephem Sulfone. *Biochemistry* **2001**, *40*, 6233−6239.

(23) Heinze-Krauss, I.; Angehrn, P.; Charnas, R. L.; Gubernator, K.; Gutknecht, E. M.; Hubschwerlen, C.; Kania, M.; Oefner, C.; Page, M. G. P.; Sogabe, S.; Specklin, J.-L.; Winkler, F. K. Structure-Based Design of Potent β-Lactamase Inhibitors. *J. Med. Chem.* **1998**, *41*, 3961−3971.

(24) Fonze, E.; Vanhove, M.; Dive, G.; Sauvage, E.; Frere, J.-M.; Charlier, P. Crystal Structures of the *Bacillus licheniformis* Bs3 Class A β-Lactamase and of the Acyl-Enzyme Adduct Formed with Cefoxitin. *Biochemistry* **2002**, *41*, 1877−1885.

(25) Frere, J.-M. Beta-Lactamases and Bacterial Resistance to Antibiotics. *Molecular Microbiol*. **1995** *16*, 385−395.

(26) Ishiguro, M.; Imajo, S. Modeling Study on a Hydrolytic Mechanism of Class A β-Lactamases. *J. Med. Chem.* **1996**, *39*, 2207−2218.

(27) Bulychev, A.; Massova, I.; Miyashitaski; Mobasherry, S. A. Nuances of Mechanisms and Their Implications for Evolution of the Versatile β-Lactamase Activity: From Biosynthetic Enzymes to Drug Resistance Factors. *J. Am. Chem. Soc.* **1997**, *119*, 7619−7625.
(28) Patera, A.; Blaszczak, L. C.; Shoichet, B. K. Crystal Structures of Substrate and Inhibitor Complexes with AmpC β-Lactamases: Possible Implications for Substrate-Assisted Catalysis. *J. Am. Chem. Soc.* **2000**, *122*, 10504−10512.
(29) Oefner, C.; D'Arcy, A.; Daly, J. J.; Gubernator, K.; Charnas, R. L.; Heinze, I.; Hubschwerfen, C.; Winkler, F. K. Refined Crystal Structure of β-Lactamase of *Citrobacter freundii* Indicates a Mechanism for β-Lactam Hydrolysis. *Nature* **1990**, *343*, 284−288.
(30) Lobkovsky, E.; Bilings, E. M.; Moews, P. C.; Rahil, J.; Pratt, R. F.; Knox, J. R. Crystallographic Structure of a Phosphonate Derivative of the *Enterobacter cloacae* P99 Cephalosporinase: Mechanistic Interpretation of a β-Lactamase Transition State Analogue. *Biochemistry* **1994**, *33*, 6762−6772.
(31) Matagne, A.; Ledent, P.; Monnaie, D.; Felici, A.; Jamin, M.; Raquet, X.; Galleni, M.; Klein, D.; Francois, I.; Frere, J. M. Kinetic Study of Interaction between BRL 42715, β-Lactamases, and D-Alanyl-D-Alanine Peptidases. *Antimicrob. Agents Chemother*. **1995**, *39*, 227−331.
(32) Bush, K.; Macalintal, C.; Rasmussen, B. A.; Lee, V. J.; Yang, Y. Kinetic Interactions of Tazobactam with β-Lactamases from all Major Structural Classes. *Antimicrob. Agents Chemother.* **1993**, *37*, 851−858.
(33) In vitro activities were determined by the microbath dilution method in accordance with NCCLS 2000. Mueller-Hinton II broth (MHBII) was used for the testing procedure. The bacterium inoculam size was 10^5 CFU/mL and the microtiter plates were incubated for 18−22 h at 35 °C.
(34) Rice, L. B.; Carias, L. L.; Hujer, A. M.; Bonafede, M.; Hutton, R.; Hoyen, C.; Bonomo, R. A. High-Level Expression of Chromosomally-Encoded SHV-1 β-Lactamase and an Outer Membrane Protein Change Confer Resistance to Ceftazidime and Piperacillin-Tazobactam in a Clinical Isolate of *Klebsiella pneumoniae*. *Antimicrob. Agents Chemother*. **2000**, *44*, 362−367.
(35) Nukaga, M.; KiKuo, T.; Yamaguchi, H.; Sawai, T. Interaction of Oxyimino β-Lactams with a Class C β-Lactamase and a Mutant with a Spectrum Extended to β-Lactams. *Antimicrob. Agents Chemother.* **1994**, *38*, 1374−1377.
(36) Otwinowski, Z.; Minor, W. Processing of X-ray Diffraction Data Collected in Oscillation Mode. *Methods Enzymol.* **1997**, *276*, 307−326.
(37) Kraulis, P. Molscript: A Program To Produce Both Detailed and Schematic Plots of Protein Structures. *J. Appl. Crystallogr*. **1991**, *24*, 946−950.
(38) Merritt, E. A.; Bacon, D. J. Raster3D: Photo-Realistic Molecular Graphics. *Methods Enzymol.* **1997**, *277*, 505−524.
(39) (a) Trapani, G.; Franco, M.; Latrofa, A.; Carotti, A.; Genchi, G.; Serra, M.; Biggio, G.; Liso, G. Synthesis, in Vitro and in Vivo Cytotoxicity and Prediction of the Intestinal Absorption of Substituted 2-Ethylcarbonyl-imidazo[2,1-b]benzothiazoles. *J. Med. Chem.* **1996**, *31*, 575−587. (b) Grandolini, G.; Ambrogi, V.; Perioli, L.; De Caprariis, P.; Palagiano, F.; Rimoli, M. G.; Lampa, E.; D'Amico, M. Synthesis and Pharmacological Activity of Imidazo[2,1-b]benzothiazole Acids. *Farmaco* **1993**, *48*, 31−43. (c) Clements-Jewery, S.; Danswan, G.; Gardner, C. R.; Mathara, S. S.; Murdoch, R.; Tully, W. R.; Westwood, R. (Imidazo[1,2-a]-pyrimidin-2-yl)phenyl Methanones and Related Compounds as Potential Nonsedative Anxiolytics. *J. Med. Chem*. **1988**, *31*, 1220−1226.

JM049680X